

Planck constraints on primordial non-Gaussianity

(Planck 2013 Results. XXIV)



Sabino Matarrese

Physics & Astronomy Dept. “G. Galilei”, Padova University - Italy

On behalf of the Planck collaboration



Primordial non-Gaussianity: a new route to falsify Inflation ...



- Strongly non-Gaussian initial conditions studied in the eighties
- New era with f_{NL} models from inflation (Salopec & Bond 1991; Gangui et al. 1994: $f_{NL} \sim 10^{-2}$; Verde et al. 1999; Komatsu & Spergel 2001; Acquaviva et al. 2002; Maldacena 2002; + many models with (much) higher f_{NL}).
- Primordial NG emerged as a new “smoking gun” of (non-standard) inflation models, which complements the search for primordial GW



Simple-minded NG model



has become reality

Many primordial (inflationary) models of non-Gaussianity can be represented in configuration space by the simple formula (Salopek & Bond 1990; Gangui et al. 1994; Verde et al. 1999; Komatsu & Spergel 2001)

$$\Phi = \phi_L + f_{NL} * (\phi_L^2 - \langle \phi_L^2 \rangle) + g_{NL} * (\phi_L^3 - \langle \phi_L^2 \rangle \phi_L) + \dots$$

where Φ is the large-scale gravitational potential (more precisely $\Phi = 3/5 \zeta$ on superhorizon scales, where ζ is the gauge-invariant comoving curvature perturbation), ϕ_L its linear Gaussian contribution and f_{NL} the dimensionless non-linearity parameter (or more generally non-linearity function). The percent of non-Gaussianity in CMB data implied by this model is

$$NG \% \sim 10^{-5} |f_{NL}|$$

$$\sim 10^{-10} |g_{NL}|$$

“non-Gaussianity = non-dog”
(Ya.B. Zel'dovich)

$< 10^{-4}$ from
CMB & LSS

$< 10^{-4}$ from
CMB & LSS



Planck 2013 results XXIV: Scientific target



- Constrain (with high precision) and/or detect primordial non-Gaussianity (NG) as due to (non-standard) inflation
- NG amplitude and shape measure deviations from standard inflation, perturbation generating processes after inflation, initial state before inflation, ...
- We test: ***local, equilateral, orthogonal*** shapes (+ many more) for the bispectrum and constrain the primordial trispectrum (test of multi-field models) parameter τ_{NL}

CMB bispectrum

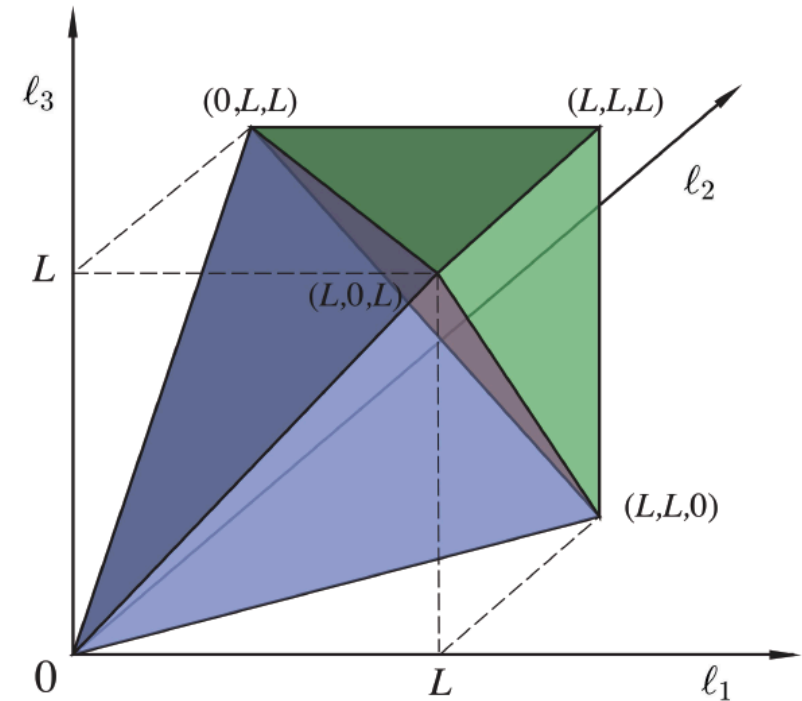
$$B_{\ell_1 \ell_2 \ell_3}^{m_1 m_2 m_3} \equiv \langle a_{\ell_1 m_1} a_{\ell_2 m_2} a_{\ell_3 m_3} \rangle$$

$$= G_{m_1 m_2 m_3}^{\ell_1 \ell_2 \ell_3} b_{\ell_1 \ell_2 \ell_3}$$

Gaunt integrals

$$G_{m_1 m_2 m_3}^{\ell_1 \ell_2 \ell_3} \equiv \int Y_{\ell_1 m_1}(\hat{n}) Y_{\ell_2 m_2}(\hat{n}) Y_{\ell_3 m_3}(\hat{n}) d^2 \hat{n}$$

$$= h_{\ell_1 \ell_2 \ell_3} \begin{pmatrix} \ell_1 & \ell_2 & \ell_3 \\ m_1 & m_2 & m_3 \end{pmatrix},$$



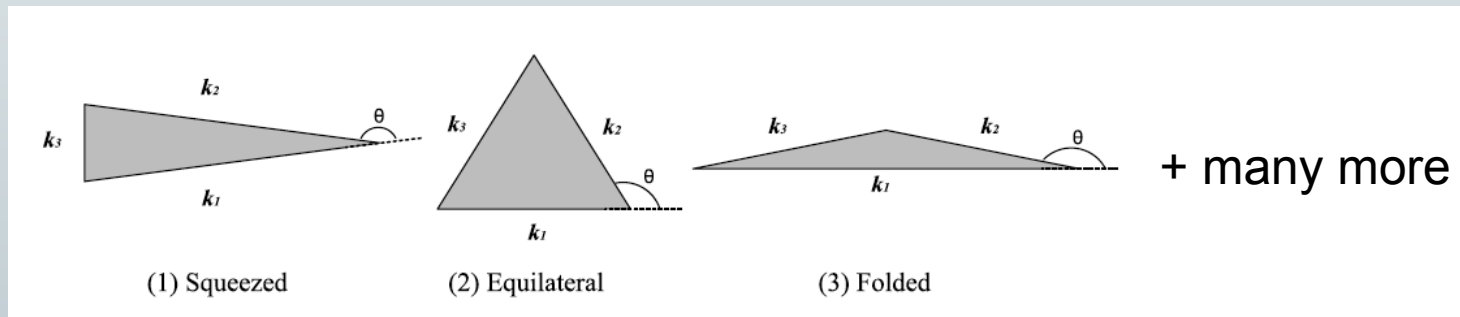
Triangle condition: $\ell_1 \leq \ell_2 + \ell_3$ for $\ell_1 \geq \ell_2, \ell_3$, +perms.

Parity condition: $\ell_1 + \ell_2 + \ell_3 = 2n$, $n \in \mathbb{N}$,

Resolution: $\ell_1, \ell_2, \ell_3 \leq \ell_{\max}$, $\ell_1, \ell_2, \ell_3 \in \mathbb{N}$.

the NG shape information

*... there are more shapes of non-Gaussianity
(from inflation) than ... stars in the sky*



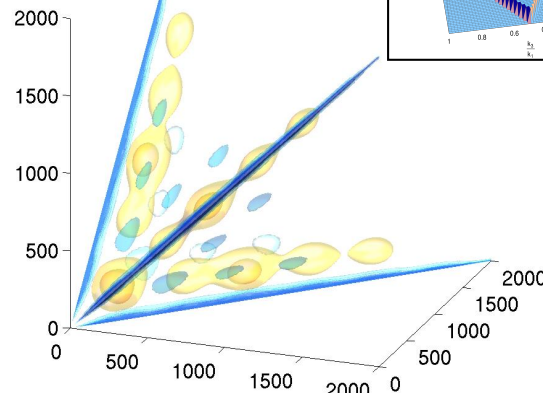


planck

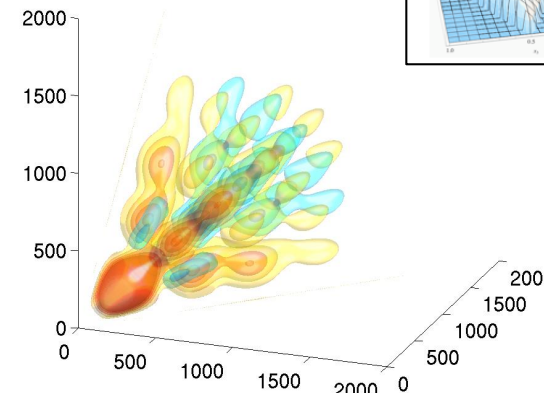
Shapes



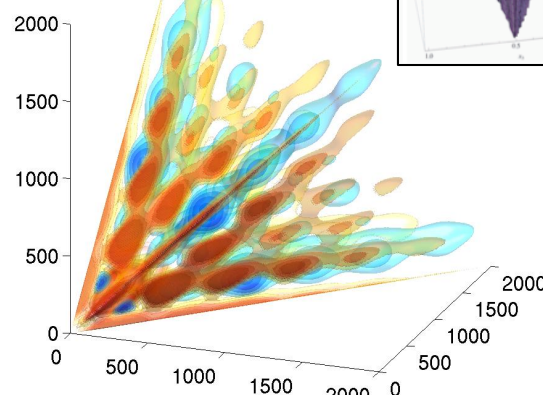
Local



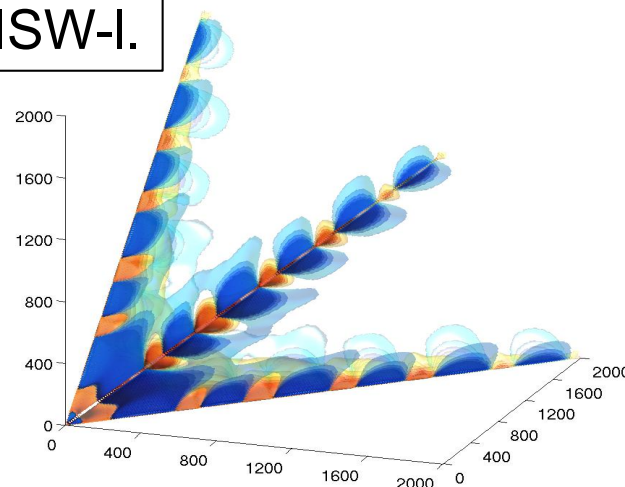
Equilateral



Orthog.



ISW-I.





Bispectrum shapes



- ***local*** shape: Multi-field models, Curvaton, Ekpyrotic/cyclic, etc. ...
- ***equilateral*** shape: Non-canonical kinetic term, DBI, K-inflation, Higher-derivative terms, Ghost, EFT approach
- ***orthogonal*** shape: Distinguishes between variants of non-canonical kinetic term, higher-derivative interactions, Galilean inflation
- ***flat*** shape: non-Bunch-Davies initial state and higher-derivative interactions, models where a Galilean symmetry is imposed. The flat shape can be written in terms of equilateral and orthogonal.

$$\hat{f}_{NL} = \frac{1}{N} \sum B_{\ell_1 \ell_2 \ell_3}^{m_1 m_2 m_3} \left[\left(C^{-1} a \right)_{\ell_1}^{m_1} \left(C^{-1} a \right)_{\ell_2}^{m_2} \left(C^{-1} a \right)_{\ell_3}^{m_3} - 3 C_{\ell_1 m_1 \ell_2 m_2}^{-1} \left(C^{-1} a \right)_{\ell_3}^{m_3} \right]$$

The theoretical template needs to be written in separable form. This can be done in different ways and *alternative implementations differ basically in terms of the separation technique adopted and of the projection domain.*

- KSW (Komatsu, Spergel & Wandelt 2003) separable template fitting + Skew-C_l extension (Munshi & Heavens 2010)
- Binned bispectrum (Bucher, Van Tent & Carvalho 2009) → see [Bartjan Van Tent talk](#)
- Modal expansion (Fergusson, Liguori & Shellard 2009) → see [Michele Liguori and Paul Shellards talks](#)

Sub-optimal estimators also applied:

Wavelet decomposition (Martinez-Gonzalez et al. 2002; Curto et al. 2009) &
Minkowski Functionals (Ducout et al. 2013) → see also [B. Wandelt talk](#)

ISW-lensing bispectrum from Planck

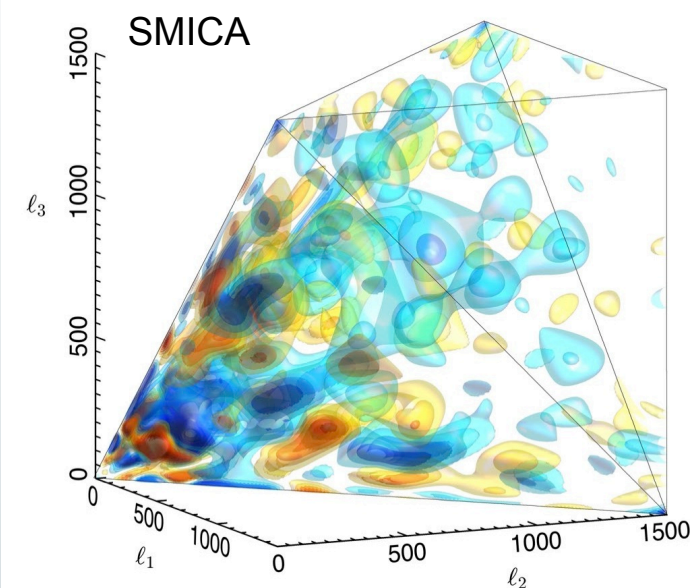
The coupling between weak lensing and Integrated Sachs-Wolfe (ISW) effects is the leading contamination to local NG. We have detected the ISW lensing bispectrum with a significance of 2.6σ (see Anna Mangilli's poster)

	SMICA	NILC	SEVEM	C-R
KSW	0.81 ± 0.31	0.85 ± 0.32	0.68 ± 0.32	0.75 ± 0.32
Binned	0.91 ± 0.37	1.03 ± 0.37	0.83 ± 0.39	0.80 ± 0.40
Modal	0.77 ± 0.37	0.93 ± 0.37	0.60 ± 0.37	0.68 ± 0.39

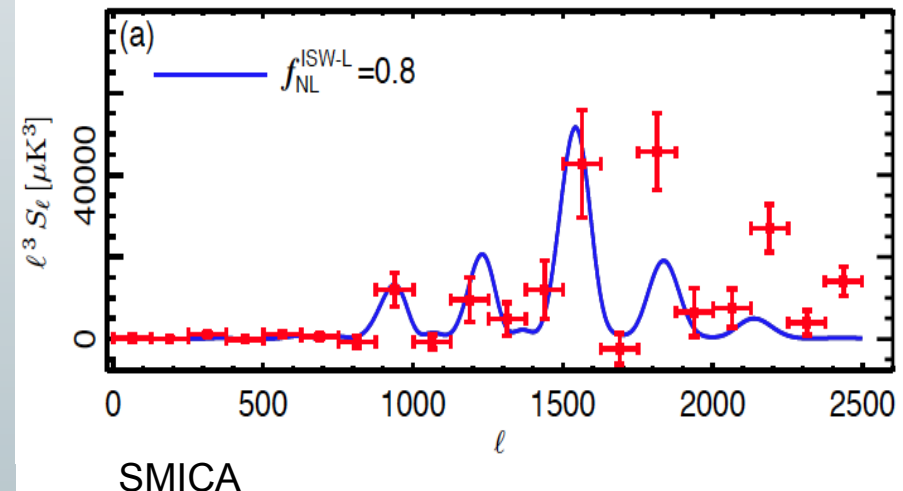
Results for the amplitude of the ISW-lensing bispectrum from the SMICA, NILC, SEVEM, and C-R foreground-cleaned maps, for the KSW, binned, and modal (polynomial) estimators; error bars are 68% CL.

	SMICA	NILC	SEVEM	C-R
Local	7.1	7.0	7.1	6.0
Equilateral	0.4	0.5	0.4	1.4
Orthogonal	-22	-21	-21	-19

The bias in the three primordial fNL parameters due to the ISW-lensing signal for the 4 component-separation methods.



Skew- C_l detection of ISW-lensing signal



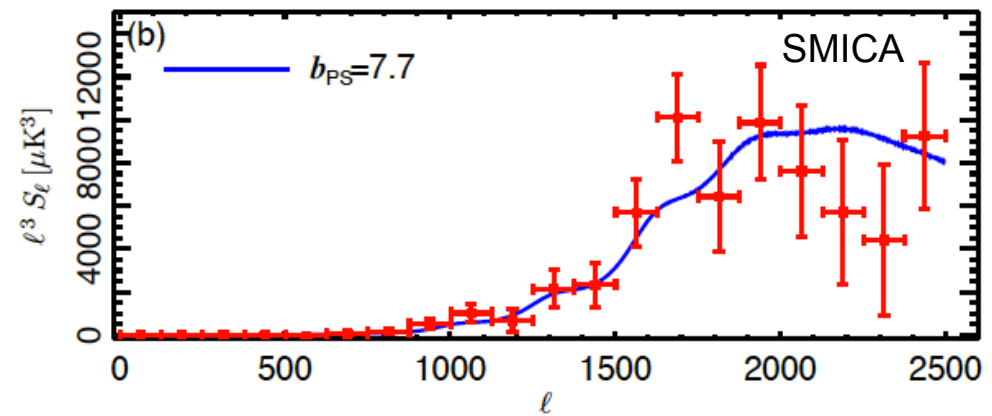
Point-sources (Poissonian) bispectrum

- Results for the amplitude of the point-source (Poisson) bispectrum (in dimensionless units of 10^{-29}) from the SMICA, NILC, SEVEM, and C-R foreground-cleaned maps, for the KSW, binned, and modal (polynomial) estimators; error bars are 68% CL. Note that the KSW and binned estimators use $\ell_{\max} = 2500$, while the modal estimator has $\ell_{\max} = 2000$.

	SMICA	NILC	SEVEM	C-R
KSW	7.7 ± 1.5	9.2 ± 1.7	7.6 ± 1.7	1.1 ± 5.1
Binned	7.7 ± 1.6	8.2 ± 1.6	7.5 ± 1.7	0.9 ± 4.8
Modal	10 ± 3	11 ± 3	10 ± 3	0.5 ± 6

Skew- C_ℓ detection of Poissonian point-source bispectrum

Skew- C_ℓ s are optimised statistics which retain information on the nature of any NG (Munshi & Heavens 2010)



Results for 3 fundamental shapes (KSW)

- Results for the f_{NL} parameters of the primordial local, equilateral, and orthogonal shapes, determined by the KSW estimator from the SMICA foreground-cleaned map. Both independent single-shape results and results marginalized over the point-source bispectrum and with the ISW-lensing bias subtracted are reported; error bars are 68% CL.

	Independent KSW	ISW-lensing subtracted KSW
SMICA		
Local	9.8 ± 5.8	2.7 ± 5.8
Equilateral	-37 ± 75	-42 ± 75
Orthogonal	-46 ± 39	-25 ± 39

- See Ben Wandelt's talk for validation o simulations and on *Planck* data
- Union Mask U73 (72% sky coverage) used throughout. Diffusive inpainting pre-filtering procedure applied.



Results for 3 fundamental shapes

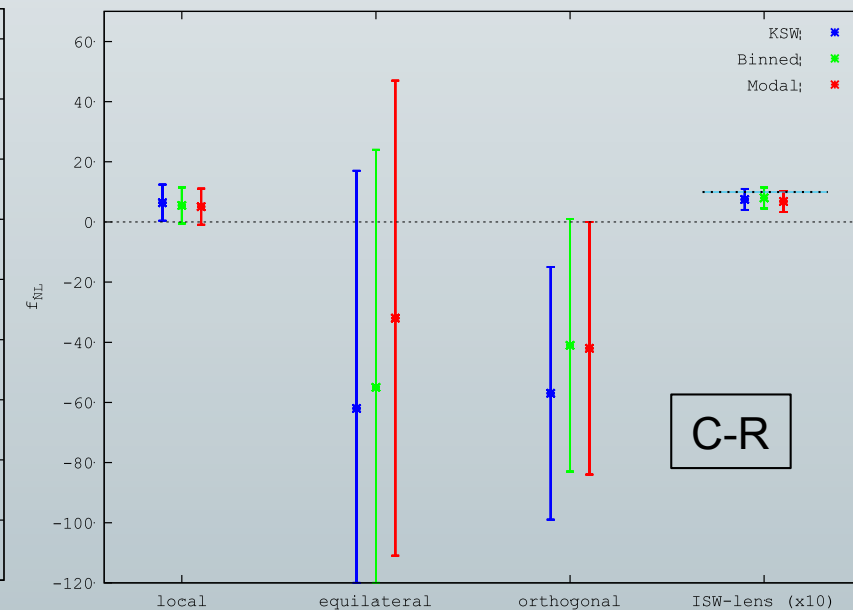
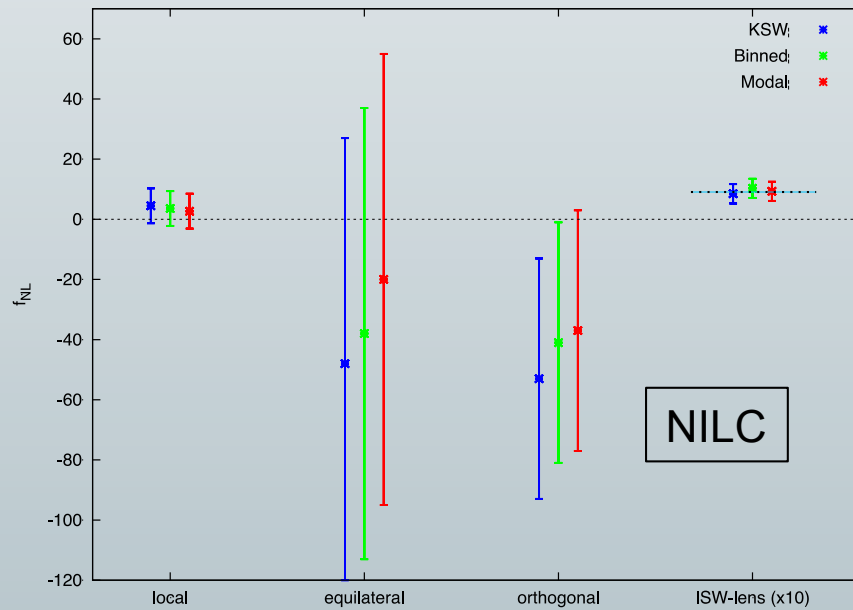
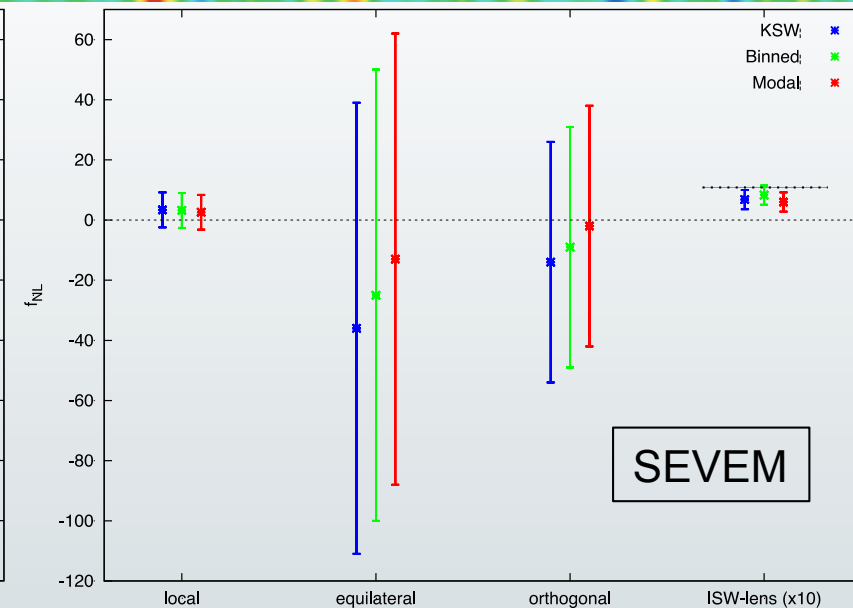
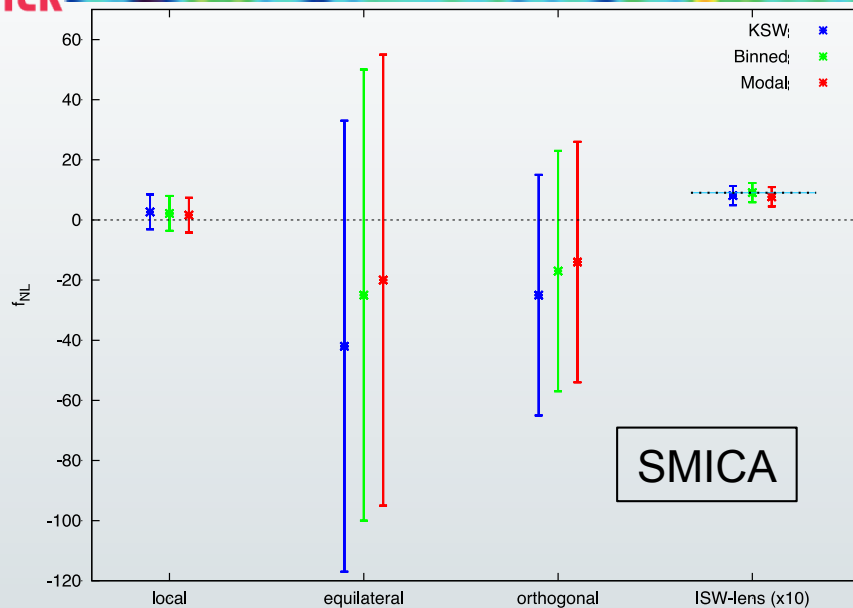


- Results for the f_{NL} parameters of the primordial local, equilateral, and orthogonal shapes, determined by the KSW, binned and modal estimators from the SMICA, NILC, SEVEM, and C-R foreground-cleaned maps. Both independent single-shape results and results marginalized over the point-source bispectrum and with the ISW-lensing bias subtracted are reported; error bars are 68% CL.

	Independent			ISW-lensing subtracted		
	KSW	Binned	Modal	KSW	Binned	Modal
SMICA						
Local	9.8 ± 5.8	9.2 ± 5.9	8.3 ± 5.9	2.7 ± 5.8	2.2 ± 5.9
Equilateral	-37 ± 75	-20 ± 73	-20 ± 77	-42 ± 75	-25 ± 73
Orthogonal	-46 ± 39	-39 ± 41	-36 ± 41	-25 ± 39	-17 ± 41
NILC						
Local	11.6 ± 5.8	10.5 ± 5.8	9.4 ± 5.9	4.5 ± 5.8	3.6 ± 5.8
Equilateral	-41 ± 76	-31 ± 73	-20 ± 76	-48 ± 76	-38 ± 73
Orthogonal	-74 ± 40	-62 ± 41	-60 ± 40	-53 ± 40	-41 ± 41
SEVEM						
Local	10.5 ± 5.9	10.1 ± 6.2	9.4 ± 6.0	3.4 ± 5.9	3.2 ± 6.2
Equilateral	-32 ± 76	-21 ± 73	-13 ± 77	-36 ± 76	-25 ± 73
Orthogonal	-34 ± 40	-30 ± 42	-24 ± 42	-14 ± 40	-9 ± 42
C-R						
Local	12.4 ± 6.0	11.3 ± 5.9	10.9 ± 5.9	6.4 ± 6.0	5.5 ± 5.9
Equilateral	-60 ± 79	-52 ± 74	-33 ± 78	-62 ± 79	-55 ± 74
Orthogonal	-76 ± 42	-60 ± 42	-63 ± 42	-57 ± 42	-41 ± 42

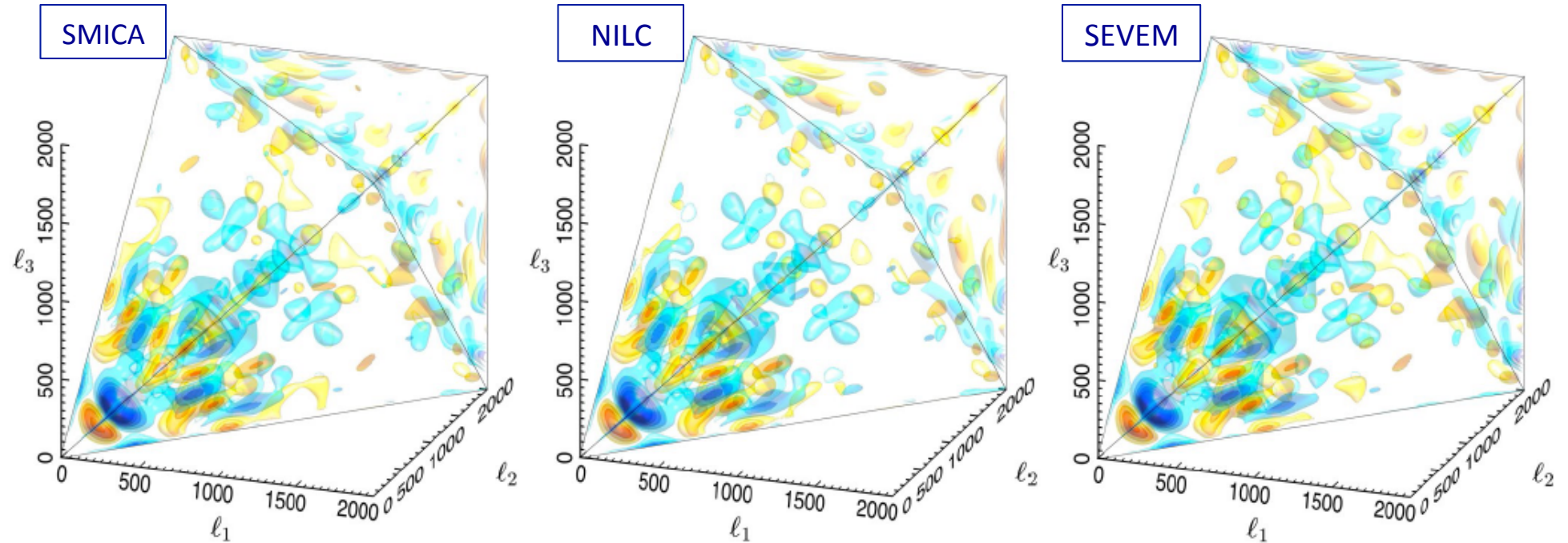


f_{NL} from Planck data



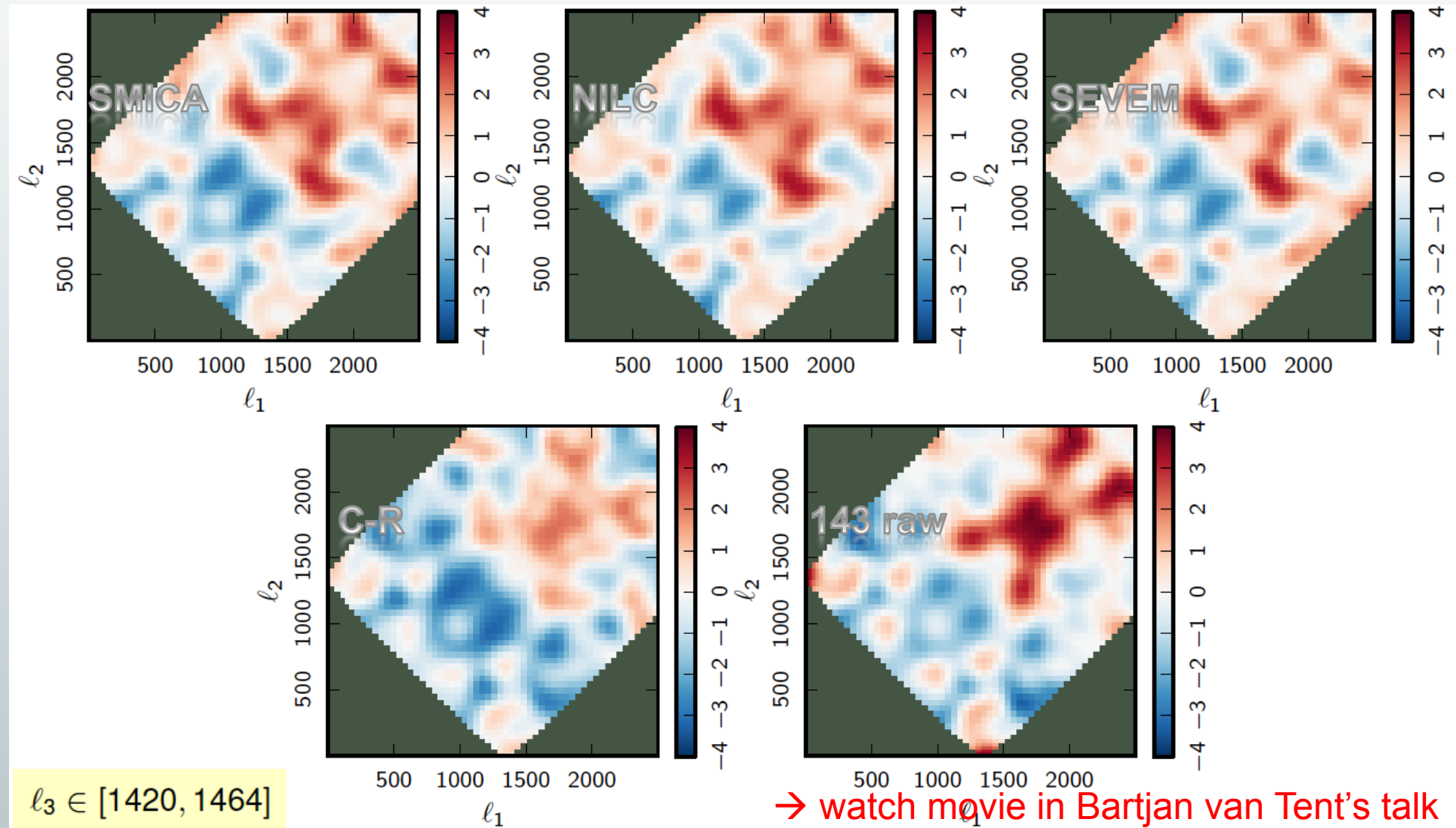
The *Planck* modal bispectrum

→ see Michele Liguori's talk



Full 3D CMB bispectrum recovered from the *Planck* foreground-cleaned maps, including SMICA, NILC and SEVEM, using hybrid Fourier mode coefficients. These are plotted in three-dimensions with multipole coordinates (ℓ_1, ℓ_2, ℓ_3) on the tetrahedral domain out to $\ell_{\max} = 2000$. Several density contours are plotted with red positive and blue negative. The bispectra extracted from the different foreground-separated maps are almost indistinguishable

The *Planck* binned bispectrum



➤ Wavelets

	Independent Wavelets	ISW-lensing subtracted Wavelets
SMICA		
Local	10 ± 8.5	0.9 ± 8.5
Equilateral	89 ± 84	90 ± 84
Orthogonal	-73 ± 52	-45 ± 52

Results for f_{NL} parameters of local, equilateral, and orthogonal shapes, determined by the suboptimal wavelet estimator (as described in Martinez-Gonzalez et al. 2002; Curto et al. 2009) from the SMICA foreground-cleaned map. Both independent single-shape results and results marginalized over the point source bispectrum and with the ISW-lensing bias subtracted are reported; error bars are 68% CL. Our current wavelets pipeline performs slightly worse in terms of error bars and correlation to primordial templates than other bispectrum estimators, but it provides an independent cross-check of other techniques.

➤ Minkowski Functionals

	f_{NL}^{local}	Source	Corresponding $\Delta f_{NL}^{\text{local}}$
Raw map	19.1 ± 19.3		–
Lensing subtracted	8.5 ± 20.5	Lensing	+10.6
Lensing+PS subtracted	7.7 ± 20.3	Point sources	+0.8
Lensing+CIB subtracted	7.5 ± 20.5	CIB	+1.0
Lensing+SZ subtracted	6.0 ± 20.4	SZ	+2.5
All subtracted	4.2 ± 20.5	All	+14.9

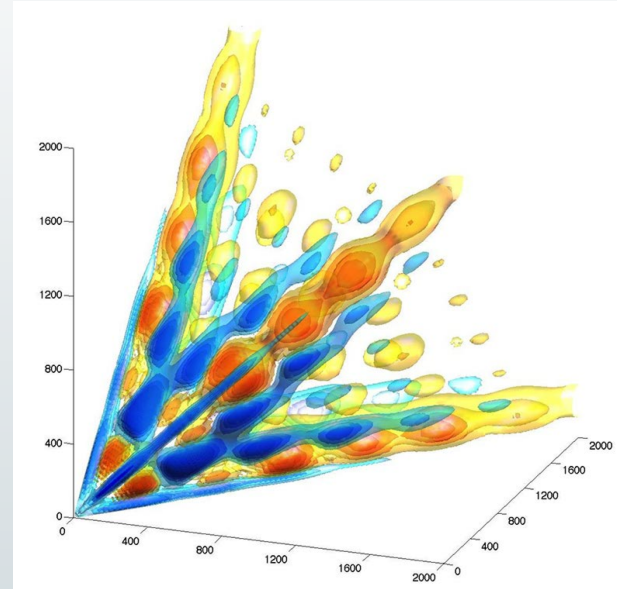
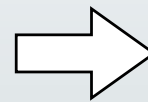
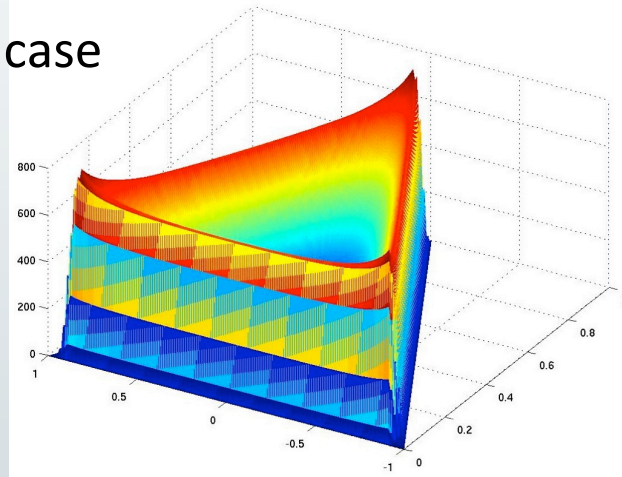
Minkowski Functionals estimates of f_{NL} local (method as in Ducout et al. 2013) obtained with MFs. Foreground and secondary effects evaluated in terms of f_{NL} local. Results for SMICA at $N_{\text{side}} = 1024$ and $L_{\text{max}} = 2000$.

Some non-standard shapes: excited initial states → see also P. Shellard's talk

Non-Bunch-Davies vacua from trans-Planckian effects or features

Five exemplar flattened models constrained

NBD case



Flattened model (Eq. number)	Raw f_{NL}	Clean f_{NL}	Δf_{NL}	σ	Clean σ
Flat model (13)	70	37	77	0.9	0.5
Non-Bunch-Davies (NBD)	178	155	78	2.2	2.0
Single-field NBD1 flattened (14)	31	19	13	2.4	1.4
Single-field NBD2 squeezed (14)	0.8	0.2	0.4	1.8	0.5
Non-canonical NBD3 (15)	13	9.6	9.7	1.3	1.0
Vector model $L = 1$ (19)	-18	-4.6	47	-0.4	-0.1
Vector model $L = 2$ (19)	2.8	-0.4	2.9	1.0	-0.1

Planck τ_{NL} constraint

- τ_{NL} power-spectrum of a modulation in the temperature fluctuation (Hanson & Lewis 2009; Pearson, Lewis & Regan 2012)

$$T(\hat{n}) \approx T_g(\hat{n})[1 + \phi(\hat{n}, r_*)] \equiv T_g(\hat{n})[1 + f(\hat{n})], \quad \tau_{\text{NL}}(L) \equiv \frac{C_L^f}{C_L^{\zeta_*}}$$

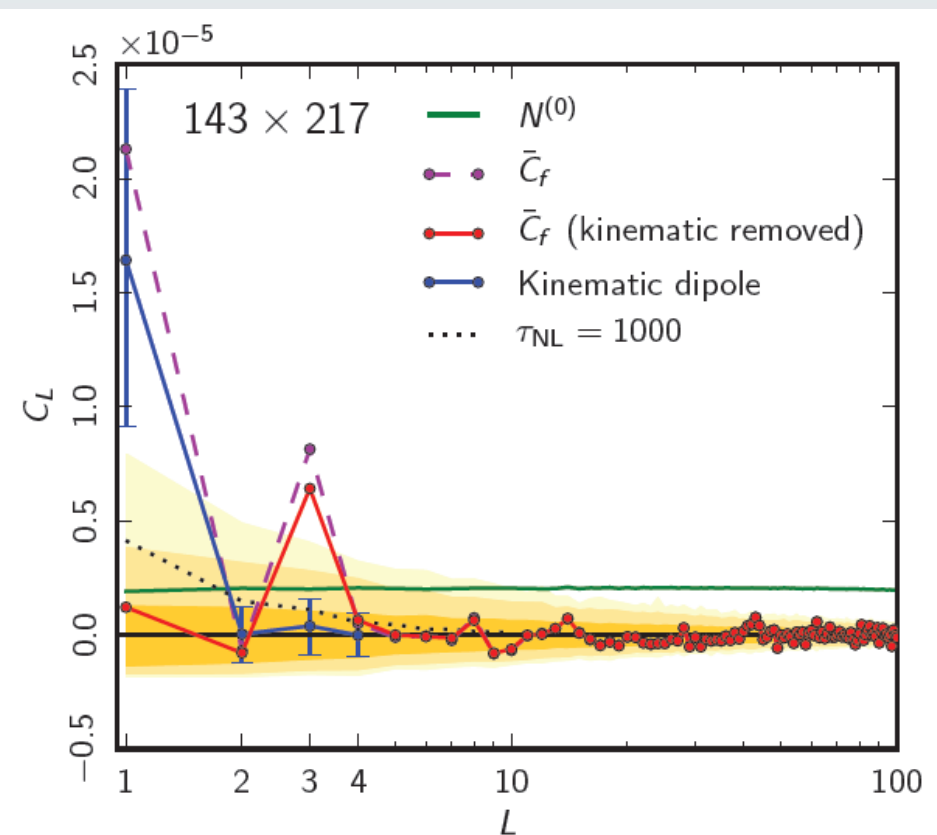
Avoid noise bias → quadratic estimator for f using noise-independent maps

Dipole signal strongly detected!
This is expected due to kinematic dipole, see

[Planck 2013 results. XXVII: “Eppur si muove”](#)

After subtracting expected kinematic dipole, modulation consistent with zero

but octopole is still anomalous compared to Gaussian simulations



Planck τ_{NL} constraint

Estimator result $\hat{\tau}_{\text{NL}} = 442$

Gaussian simulations:

$$-452 < \hat{\tau}_{\text{NL}} < 835 \text{ at 95% CL} (\sigma_{\tau_{\text{NL}}} \approx 335)$$

Consistent with Gaussian null hypothesis (octopole has small weight)

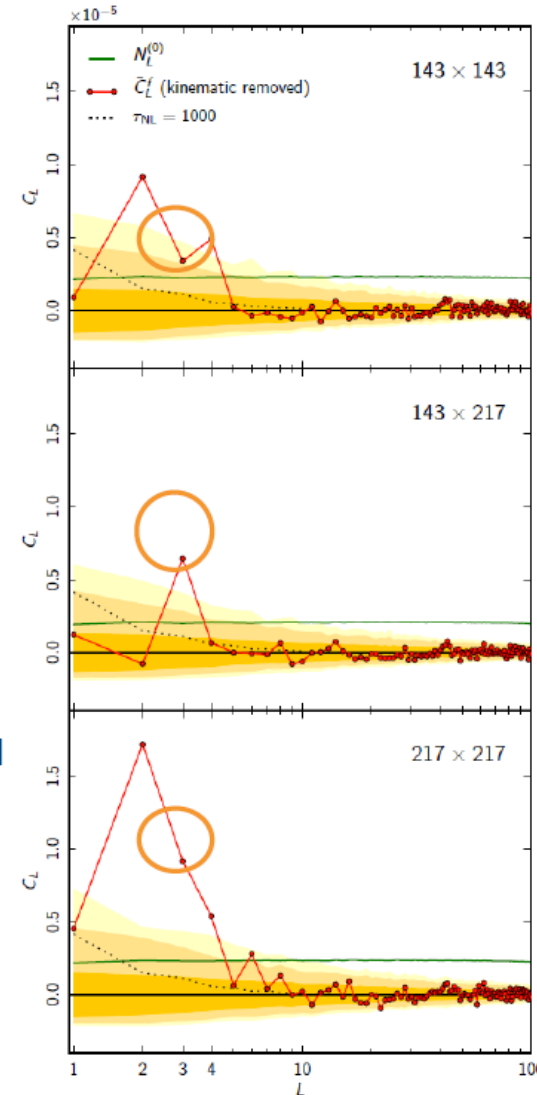
Note: signal most $L < 5$ - small number of modes

- Skewed distribution
- Upper limits weaker than you might expect

Conservative upper limit, allowing octopole to be physical using Bayesian posterior

$$\tau_{\text{NL}} < 2800 \text{ at 95% CL}$$

Octopole signal varies between frequencies:
(large auto-quadrupole expected from noise bias)



Conclusions I

- We have detected the Integrated-Sachs-Wolfe-lensing bispectrum, as expected in the Λ CDM scenario.
- We have derived constraints on early-Universe scenarios that generate primordial NG, including general single-field models of inflation, excited initial states (non-Bunch-Davies vacua), and directionally-dependent vector models.
- We have provided an initial survey of scale-dependent feature and resonance models. These results bound both general single-field and multi-field model parameter ranges, such as the speed of sound, $c_s \geq 0.02$ (95% CL), in an effective field theory parametrization ($c_s \geq 0.07$ for DBI inflation), and the curvaton decay fraction $r_D \geq 0.15$ (95% CL).
- We have constrained the amplitude of the four-point function in the local model $\tau_{NL} < 2800$ (95% CL), using an estimator introduced by Hanson & Lewis 2009, which is based on large-scale modulation of small-scale power.



Conclusions II



- The **simplest** inflation models (single-field slow-roll, standard kinetic term, BD initial vacuum state) are favoured by *Planck* data
- Multi-field models are not ruled out but also not detected.
- Ekpyrotic/cyclic models either ruled out or under severe pressure
- *Taken together, these constraints represent the highest precision tests to date of physical mechanisms for the origin of cosmic structure.*



Future prospects



➤ short term goals

- Improve f_{NL} limits with polarization & full data
- Look for more non-Gaussian shapes, scale-dependence, etc. ...
- constrain g_{NL}

➤ long terms goals

- reconstruct inflationary action: are models with large g_{NL} and small f_{NL} preferred by laws of nature?
- if (quadratic) NG turns out to be small for all shapes (?) go on and search for $f_{NL} \sim 1$ non-linear GR effects and second-order radiation transfer function contributions
- what about intrinsic ($f_{NL} \sim 10^{-2}$) NG of standard inflation? CMB polarization + LSS + 21cm background + ???

The scientific results that we present today are a product of the Planck Collaboration, including individuals from more than 100 scientific institutes in Europe, the USA and Canada



Planck is a project of the European Space Agency, with instruments provided by two scientific Consortia funded by ESA member states (in particular the lead countries: France and Italy)

with contributions from NASA (USA), and telescope reflectors provided in a collaboration between ESA and a scientific Consortium led and funded by Denmark.